Acupuncture attenuates renal interstitial fibrosis via the TGF-β/Smad pathway

ZHENG ZUO[1], PEIDONG HUANG[2], YUNWU JIANG[2], YI ZHANG[3] And MIANSHENG ZHU[1]

[1]Acupuncture and Massage College, Beijing University of Chinese Medicine, Beijing 100029;
[2]Acupuncture and Massage Rehabilitation College, Yunnan University of Chinese Medicine, Kunming, Yunnan 650500;
[3]Acupuncture and Moxibustion Department, Zibo Hospital of Traditional Chinese
Medicine of Shandong Province, Zibo, Shandong 255300, P.R. China

Abstract. Acupuncture is one of the most useful tools in complimentary medicine, and has demonstrated potential value for treating chronic renal failure (CRF). However, the underlying mechanisms for its therapeutic effect remain unknown. In the present study, the effects of acupuncture on renal interstitial fibrosis (RIF) were explored in a rabbit model of CRF. Rabbits were assigned to the following five groups: sham, model, losartan potassium (Posi), acupuncture (Acup) and acupuncture+inhibitor (Acup+Inhib) groups. The CRF rabbits were administered a drug or/and acupuncture on Shenshu, Mingmen and Pishu. The body weights, urine protein, serum creatinine (SCr) and blood urea nitrogen (BUN) levels of the rabbits were measured. Transforming growth factor β (TGF-β), integrin-linked kinase (ILK) and Smad3 expression were detected by qRT-PCR. Tumor necrosis factor-α (TNF-α) and endothelial nitric oxide synthase (eNOS) expression were analyzed by western blot methods. The concentrations of TGF-β, IL-8, TNF-α and IL-1β in blood serum were detected using ELISA kits. In addition, pathological characteristics of the rabbit tissues were evaluated by H&E and Masson's trichrome staining methods, and TGF-β expression was detected by immunohistochemistry (IHC) assays. Results showing decreased body weights and increased urine protein, SCr and BUN levels confirmed that the CRF model had been successfully constructed. It was also found that acupuncture significantly reduced the levels of TNF-α, Smad3, ILK and TGF-β expression, dramatically decreased the concentrations of TGF-β, IL-8, TNF-α and IL-1β in blood serum, and significantly increased eNOS expression in the CRF model rabbits by affecting the TGF-β/Smad signaling pathway. In addition, it was demonstrated that acupuncture could relieve RIF by affecting the TGF-β/Smad pathway. These observations indicate that acupuncture may be useful for treating CRF, and suggest the TGF-β/Smad pathway as a target for CRF therapy.

Introduction

Chronic kidney disease (CKD) has become one of the major diseases that threatens public health worldwide, and causes an enormous amount of suffering and economic expense (1). The prevalence of CKD has reached epidemic proportions, as it currently affects 10-13% of the populations in Taiwan, Japan, China, Canada, India and the USA (2). More than 100 million individuals rely on dialysis to survive worldwide, and this number increases at a mean annual rate of 8% (3). Moreover, increasing numbers of young people suffer from CKD, with the youngest patient being <10 years of age (4). Therefore, there is a critical and urgent need to reduce the frequency of kidney injury and protect the kidneys from all types of kidney disease.

Renal interstitial fibrosis (RIF) is a kidney disorder characterized by dilated kidney tubules and interstitial fibrosis (5). Studies have indicated that the degree of RIF indicates the degree of kidney damage, which makes RIF an important factor when establishing a prognosis for patients with kidney diseases (6-8). RIF is also an important factor for predicting CKD, which is currently increasing in prevalence (9,10). Therefore, to delay the development of CKD, it is of great importance that we identify biomarkers for CKD, and also explore methods for preventing and treating RIF. The occurrence and development of RIF are influenced by numerous factors, including renal tubular epithelial cell apoptosis, inflammation, cytokines, oxidative stress, fibroblast proliferation and activation, the production of vasoactive substances, and an imbalance between extracellular matrix synthesis and degradation (11-14). Due to the large number of pathologic mechanisms for RIF, we speculate that additional unknown mechanisms and biomarkers for RIF remain to be discovered. Renal fibrogenesis is related to multiple cellular events and molecular mediators (15). Among the fibrogenic factors that regulate the renal fibrotic process, transforming growth factor β (TGF-β) has long been considered as a

Correspondence to: Dr Miansheng Zhu, Acupuncture and Massage College, Beijing University of Chinese Medicine, 11 North Third Ring Road, Chaoyang, Beijing 100029, P.R. China
E-mail: zhumiansheng@yeah.net

central mediator of the fibrotic response (16). TGF-β exerts its biological effects mainly via its downstream Smad signaling molecules (17,18). The TGF-β/Smad3 signal is transduced by type I and type II serine/threonine kinase receptors found in the cell membrane (19). TGF-β1 binds to its type II receptor, and this complex then forms a dimer with the type I receptor, resulting in phosphorylation and activation of the type I receptor. The activated type I receptor phosphorylates Smad2 and/or Smad3, which then heterodimerizes with Smad4 and subsequently translocates into the nuclei, where it regulates the transcription of TGF-β-target genes (20). Some adaptor proteins, including Smad anchor for receptor activation (SARA), disabled-2 (DAB2), ELF-spectrin and endofin have been reported to facilitate TGF-β signaling by linking Smad2/Smad3 to the receptor complex (21). However, the pathogenic molecular mechanisms involved in RIF are poorly understood.

Acupuncture is a traditional Chinese therapy with thousands of years of history, and is now recognized and accepted as a medical therapy worldwide (22). As a green complementary and alternative therapy, acupuncture has demonstrated significant effects on many diseases, especially on functional diseases (23-25). However, the mechanism by which acupuncture exerts its effects remains elusive. This limits our progress in understanding acupuncture and how to optimize its clinical effects. Therefore, clarifying the mechanism by which acupuncture affects RIF would be valuable for further development in the field of acupuncture therapy.

In the present study a rabbit model of CRF was utilized to explore the renal protective effect of acupuncture and the underlying mechanism for that effect. Our results provide a theoretical basis for the clinical use of acupuncture in treating CKD.

Materials and methods

Animal preparation. A total of 30 6-month-old healthy male adult New Zealand White rabbits (body weight, 1.8-2.2 kg) were obtained from the Experimental Animal Center of Yunnan College of Traditional Chinese Medicine. On arrival, the rabbits were allowed to acclimatize to their new environment for one week before any procedure was performed. The rabbits were fed separately, and had free access to 200 g of food and water in an undisturbed and clean environment. The animals were housed in a room that had a 12-h light/dark cycle, and was maintained at a temperature of 18-24°C and a relative humidity ranging from 40 to 70%. All experiments were performed in accordance with the recommendations provided in Guidelines for the Care and Use of Laboratory Animals, and the study protocol was approved by the Animal Research Committee of Yunnan College of Traditional Chinese Medicine (Cumming, China). Animals were anesthetized by pentobarbital (i.v., 40 mg/kg) and sacrificed by exsanguination (blood volume, ~85 ml each).

Chronic renal failure (CRF) model. The CRF model was created by gavaging the rabbits with adenine for 3 weeks, as previously described (26). Adenine (purity >98%; FW: 135.14) was purchased from Guangzhou Weijia Technology Co., Ltd. (Guangzhou, China). New Zealand White rabbits

(n=6) in the control group were gavaged with an equivalent amount of distilled water (10 ml/kg/day) for 21 days. The other New Zealand White rabbits (n=24) were used to construct the CRF rabbit model. In brief, the rabbits were gavaged with 25% adenine (150 mg/kg/day) dissolved in normal saline for 21 consecutive days. After 21 days, their kidney function, blood pressure and urinary protein levels were measured.

Renal function analysis. Serum creatinine (SCr) and blood urea nitrogen (BUN) were detected with an IDEXX Catalyst One Chemistry Analyzer (IDEXX Laboratories, Inc., Westbrook ME, USA).

Experiments and acupuncture procedure. The CRF rabbits were randomly assigned to a CRF model group (n=6), a losartan potassium positive control group (Posi, CRF model treated with losartan potassium; n=6), an acupuncture group (Acup, CRF model administered acupuncture; n=6), or an acupuncture+SB 431542 group (Acup+inhibitor, CRF model administered acupuncture and SB 431542; n=6). Rabbits in the CRF model group were fed a standard diet without drugs. CRF rabbits in the Posi group were fed a standard diet and also received 2.33 mg/kg/day of losartan potassium (100 mg/tablet, produced by Hangzhou MSD Pharmaceutical Co., Ltd., Hangzhou, China) by gavage, once a day. CRF rabbits in the acupuncture group were fed a standard diet and were stimulated by acupuncture treatment (Shenshu, Mingmen and Pishu) for 30 min, once a day. CRF rabbits in the Acup+inhibitor group were fed a standard diet and received SB 431542 (2.5 mg/kg/2 days; Tocris Bioscience, Bristol, UK) by intraperitoneal injection. Acupuncture was administered with a sterilized acupuncture needle (diameter: 0.25 mm, length: 40 mm; TCM Supply Co., Ltd. Yokohama, Japan). During acupuncture, sterilized acupuncture needles were gently inserted to a depth of 5 mm below the surface of acupuncture points at Shenshu, Mingmen and Pishu. The treatments were continued for 36 days, and each animal's diet, urine volume, mental state, hair color and weight were monitored.

Histopathological analysis. The samples obtained from all groups were washed and then fixed in 4% paraformaldehyde (Sigma-Aldrich; Merck KGaA, Darmstadt, Germany) for 30 min. Next, the tissues were dehydrated in a gradient alcohol series, treated in xylene, imbedded with paraffin, and cut into 4-μm sections. For the hematoxylin and eosin (H&E) staining assay, the sections were stained with hematoxylin for 5 min and then dehydrated with 70 and 90% ethanol; after which, they were treated with eosin for 3 min. Each section was then evaluated under a light microscope (CX41; Olympus Corporation, Tokyo, Japan; magnification, x200). For Masson's trichrome staining, the sections were stained with reagents in a Masson's Trichrome Stain kit (Sigma-Aldrich; Merck KGaA) according to the manufacturer's instructions. Masson staining results were quantified using Image-Pro Plus (version 6.0; Media Cybernetics, Inc., Rockville, MD, USA). Briefly, integral optical density of three areas-of-interest was assessed for staining quantification.

Real-time quantitative PCR (qPCR) assay. TRIzol reagent (Invitrogen; Thermo Fisher Scientific, Inc., Waltham, MA,

USA) was used to extract total RNA from the tissue samples of all groups as described in the manufacturer's instructions. RNA concentrations were determined by measuring absorbance at 260/280 nm. cDNA was obtained by using a First Strand cDNA Synthesis kit (Thermo Fisher Scientific, Inc.). Specific genes were amplified by using SYBR-Green PCR Master Mix (Takala Biotechnology, Co., Ltd., Dalian, China) and an ABI 7500 Real-time PCR system (Applied Biosystems; Thermo Fisher Scientific, Inc.). β-actin served as an endogenous housekeeping gene. Amplification data were analyzed using the $2^{-\Delta\Delta Cq}$ method (27). The following primers were used for amplification: TGF-β: 5'-CAAGTGGACATC AACGGGA-3' (forward) and 5'-GCAGAAGTTGGCGTG GTAG-3' (reverse); Smad3: 5'-GAAGGATGAGGTTTGCGT GA-3' (forward) and 5'-GGATGGAATGGCTGTAGTCGT-3' (reverse); ILK: 5'-TCACCCAACCCTCATTACG-3' (forward) and 5'-TCATCAATCATTACACTACGGCTAT-3' (reverse); β-actin: 5'-CCAGGTCATCACCATCGG-3' (forward) and 5'-TGTCCACGTCGCACTTCA-3' (reverse).

Western blot assays. The total proteins were extracted from all groups of tissue samples by using a radio-immunoprecipitation assay (RIPA) buffer (Beyotime Institute of Biotechnology, Shanghai, China). The concentration of total protein in each sample was measured by using a protein reagent (Bio-Rad Laboratories, Hercules, CA, USA). Next, aliquots of total protein (30 μg per sample) were separated by electrophoresis on 10% sodium dodecyl sulfate-polyacrylamide gels, and the protein bands were transferred onto polyvinylidene fluoride (PVDF) membranes (cat. no. IPVH00010; Millipore, Burlington, MA, USA). The membranes were then blocked with 5% non-fat dry milk for 1 h, and subsequently incubated overnight at 4°C with specific primary antibodies. After being washed, the membranes were incubated with a horseradish peroxidase-conjugated secondary antibody (1:2,000, cat. no. ab97057; Abcam, Cambridge, UK) at room temperature for 1.5 h. The immunoprecipitated proteins were detected by using an enhanced chemiluminescence substrate kit that was included in an enhanced chemiluminescence detection system (Amersham Biosciences Inc., Piscataway, NJ, USA). The primary antibodies were anti-TNF-α (dilution 1:1,000; cat. no. ab6671; Abcam), anti-Smad3 (dilution 1:1,000; cat. no. ab84177; Abcam), anti-ILK (dilution 1:1,000; cat. no. ab227154; Abcam), anti-TGF-β (dilution 1:1,000; cat. no. ab92486; Abcam), anti-eNOS (dilution 1:1,000; cat. no. ab76198; Abcam) and anti-GAPDH (dilution 1:3,000, cat. no. ab9485; Abcam).

Enzyme-linked immunosorbent assay (ELISA). Samples of blood from the right common carotid artery of each rabbit were collected into anticoagulant tubes and centrifuged. TGF-β, IL-8, TNF-α and IL-1β were measured by using specific ELISA kits according to the manufacturer's instructions. The ELISA kits used in the present study were for TGF-β (cat. no. CSB-E06900Rb; Cusabio, Wuhan, China), IL-8 (cat. no. SB-E13942Rb; Cusabio), TNF-α (cat. no. CSB-E06998Rb; Cusabio) and IL-1β (cat. no. E-EL-RB0385c; Elabscience Biotechnology Co., Ltd., Wuhan, China).

Immunohistochemistry (IHC) assays. The tissues in all groups were fixed in 4% formalin (cat. no. SF100-20; Thermo Fisher Scientific, Inc.), embedded in paraffin, and cut into 4-μm thick sections. The sections were then deparaffinized, rehydrated and treated with 10 mM citrate buffer for 5 min at 100°C; after which, they were incubated with 10% fetal bovine serum (FBS) for 2 h at 37°C. Next, the sections were incubated overnight with anti-TGF-β (dilution 1:25; cat. no. ab92486; Abcam) at 4°C. After being washed with phosphate-buffered saline (PBS), the sections were incubated with an anti-rabbit secondary antibody (cat. no. ab150077; Abcam) for 2 h at room temperature. The immunostained tissues were then photographed under a light microscope (CX41; Olympus Corporation).

Statistical analysis. Each experiment was repeated at least 3 times, and results represent the mean ± standard deviation (SD). Student's t-test was used in data analysis between two groups. Statistical analyses of multiple groups were performed using the one-way analysis of variance (ANOVA) followed by post-hoc Tukey's test through IBM SPSS Statistics for Windows (version 23.0 software; IBM Corp, Armonk, NY, USA). P-values <0.05 were considered statistically significant.

Results

General condition of the experimental animals. In the present study, no rabbit in any group died, and no abnormalities of feeding or activity were observed among rabbits in the control group. However, some rabbits in the other groups displayed loss of appetite, lethargy, slowed mobility and weight loss. Rabbits in the model group displayed the most significant symptoms.

Comparison of renal function in the control and CRF model groups. Our chronic renal failure (CRF) model was created by gavaging rabbits with adenine for 3 weeks. In this study, the base line body weights, urine protein, SCr and BUN levels of all the rabbits were similar prior to establishment of the CRF model. After treatment, there were no significant changes in body weight, urine protein, SCr and BUN levels of rabbits in the control group when compared with the pre-treatment values. While the mean body weight in the model group after treatment was significantly lower than that in the control group (P<0.05; Fig. 1A), the urine protein levels in the model group were significantly higher than those in the control group (P<0.05; Fig. 1B). Furthermore, the SCr and BUN levels in the model group were also significantly higher than those in the control group (both P<0.05; Fig. 1C and D, respectively). These findings indicated that the CRF model had been successfully created.

Acupuncture attenuates kidney fibrogenesis and pathological changes in the CRF model rabbits. To explore how acupuncture affects RIF, H&E and Masson's trichrome staining were performed to evaluate morphological features of the renal tissues. As shown in Fig. 2A, the sizes of the glomeruli in the model group were dramatically decreased, and the glomeruli displayed features of patchy tubulointerstitial injury, such as a fuzzy boundary. However, these features were absent in the Posi control group, and both the
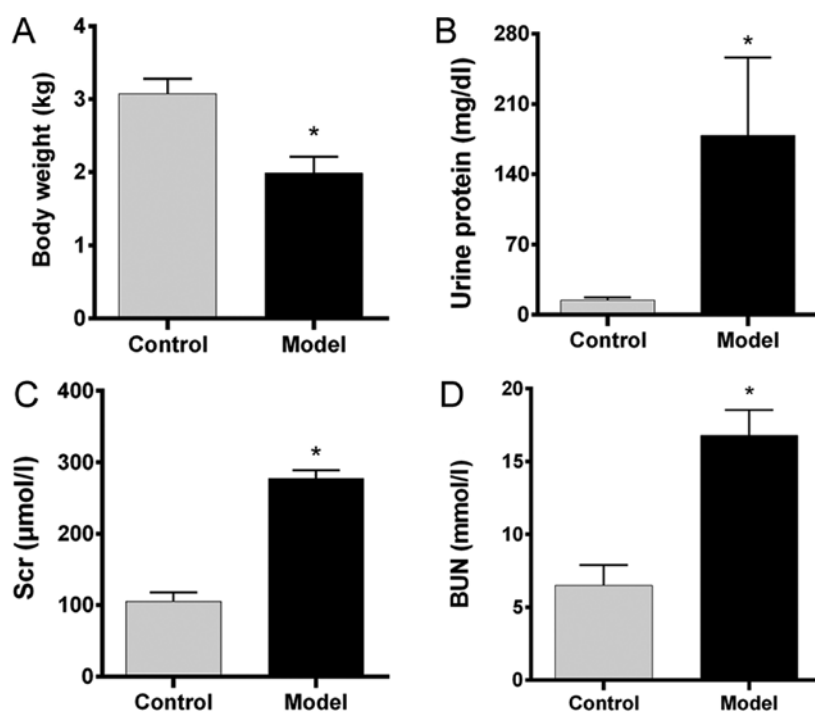
Figure 1. Comparison of renal function in the control and CRF model groups. (A) Body weight, (B) urine protein, (C) SCr and (D) BUN were measured in the control group and model group, respectively; *P<0.05 vs. control. SCr, serum creatinine; BUN, blood urea nitrogen.
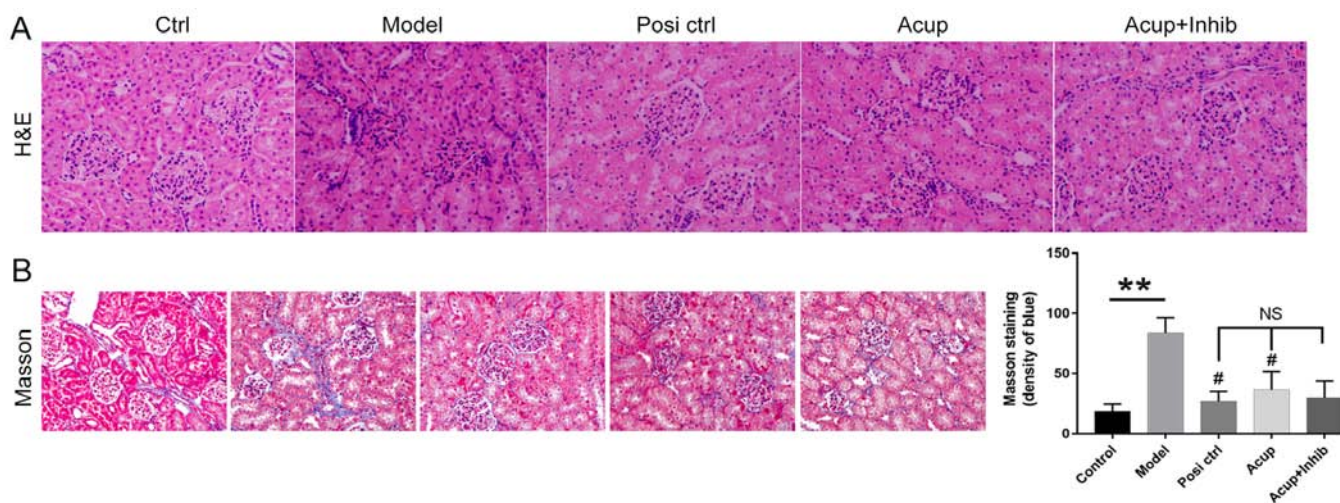

Figure 2. Acupuncture attenuates pathological characteristics and fibrogenesis in the kidney. The pathological characteristics of kidney tissues were examined by (A) H&E and (B) Masson trichrome staining assays. Original magnification, x200; Severe fibrosis (blue color). **P<0.01 vs. Control, #P<0.05 vs. Model. NS, not significant; H&E, hematoxylin and eosin. Groups: Ctrl, control group, Model, CRF model group; Posi ctrl, a losartan potassium positive control group; Acup, CRF model administered acupuncture; Acup+Inhib, CRF model administered acupuncture and SB 431542.

losartan potassium and acupuncture groups had glomeruli of significantly increased sizes. Acupuncture was able to attenuate these symptoms. As shown in Fig. 2B, interstitial fibrosis was observed more often in the model group than in the control group, and the symptoms were attenuated in the animals treated with losartan or acupuncture. Additionally, we found that the fibrogenesis was even further attenuated by TGF-β inhibitor (SB 431542) administration without significant difference (Fig. 2B).

Acupuncture downregulates TNF-α, Smad3, ILK and TGF-β expression, and upregulates eNOS in the CRF model via *the TGF-β/Smad pathway*. To explore the mechanism by which acupuncture affects RIF, New Zealand White rabbits were assigned to a control group, a CRF model group, a losartan potassium (Posi) group, an acupuncture (Acup) group, and an acupuncture+SB 431542 (Acup+inhibitor) group, respectively. As shown in Fig. 3A and B, the mRNA (Fig. 3A) and proteins (Fig. 3B) expression levels of TNF-α, Smad3, ILK and TGF-β expression were significantly upregulated in the model group when compared with the control group; TNF-α, Smad3, ILK and TGF-β expression levels were markedly downregulated in the Posi group and Acup group when compared with the model group; TNF-α
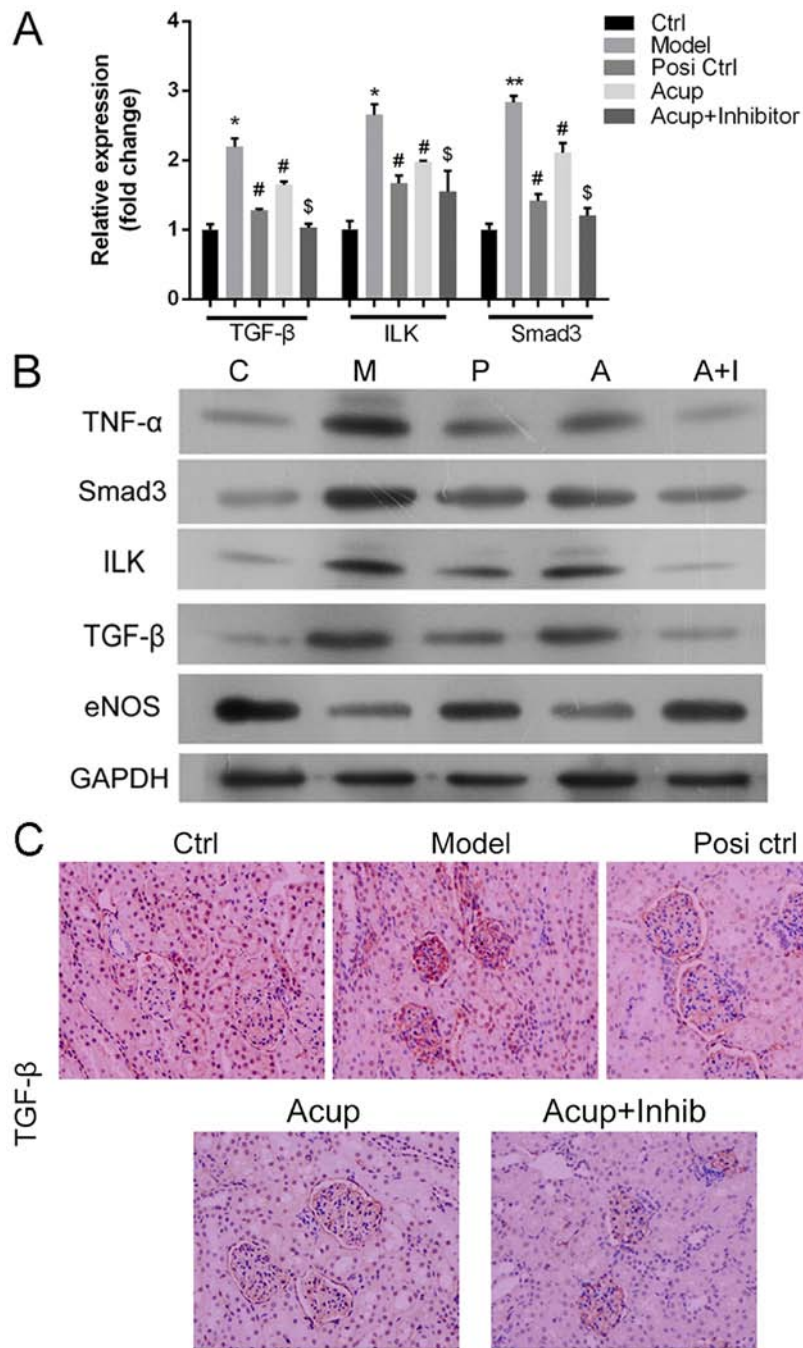
Figure 3. Acupuncture downregulates TNF-α, Smad3, ILK and TGF-β expression and upregulates eNOS in the CRF model via the TGF-β/Smad pathway. (A) qRT-PCR assays were performed to measure the expression of mRNA for TGF-β, ILK and Smad3 in all groups. *$P<0.05$, **$P<0.01$ vs. the control group; #$P<0.05$ vs. the model group; $$P<0.05$ vs. the Acup group. (B) Western blot assays were used to analyze the levels of TNF-α, Smad3, ILK, TGF-β and eNOS protein expression in all groups. GAPDH served as an internal reference. (C) TGF-β expression was detected by an IHC assay. All H&E, Masson trichrome and IHC assays (Original magnification, x200). Positive signal (blue color). TNF-α, tumor necrosis factor-α; ILK, integrin-linked kinase; TGF-β, transforming growth factor β; eNOS, endothelial nitric oxide synthase; IHC, immunohistochemistry; H&E, hematoxylin and eosin. Groups: Ctrl or C, control group, Model or M, CRF model group; Posi ctrl or P, a losartan potassium positive control group; Acup or A, CRF model administered acupuncture; Acup+Inhib or A+I, CRF model administered acupuncture and SB 431542.

and Smad3 expression were significantly decreased in the Acup+inhibitor group when compared with the Acup group ($P<0.05$ or $P<0.01$), while the levels of ILK and TGF-β expression did not significantly change. In addition, we also found that eNOS expression was markedly downregulated in the model group when compared with the control group; eNOS expression was dramatically upregulated in the Posi group and Acup group when compared with the model group;

and eNOS expression was significantly increased in the Acup+inhibitor group when compared with the Acup group (Fig. 3A and B).

TGF-β expression was detected by an IHC assay, and the results showed that TGF-β was rarely found in the control group, but was highly expressed in renal tissues (mainly in injured tubulointerstitium and renal tubular epithelial cells). It was also found that TGF-β expression was markedly
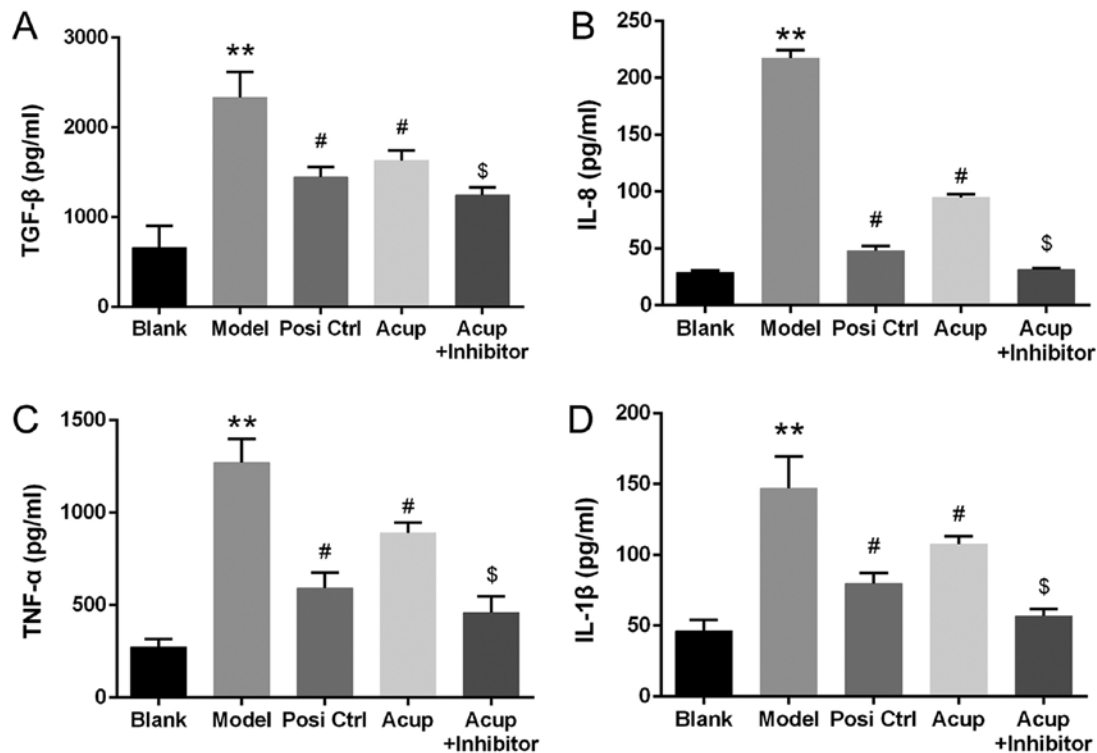
Figure 4. Acupuncture decreases TGF-β, IL-8, TNF-α and IL-1β expression in the CRF model via the TGF-β/Smad pathway. The concentrations of (A) TGF-β, (B) IL-8, (C) TNF-α and (D) IL-1β in serum samples of the mice were measured by ELISA assays in all groups. **P<0.01 vs. the control group, #P<0.05 vs. the model group, $P<0.05 vs. the Acup group. TGF-β, transforming growth factor β; IL-8, interleukin 8; TNF-α, tumor necrosis factor-α; IL-1β, interleukin-1β; CRF, chronic renal failure. Groups: Blank, control group, Model, CRF model group; Posi Ctrl, a losartan potassium positive control group; Acup, CRF model administered acupuncture; Acup+Inhibitor, CRF model administered acupuncture and SB 431542.

reduced in the Posi and Acup groups relative to its expression in the model group. Furthermore, TGF-β expression was also dramatically reduced in the Acup+inhibitor group when compared with its expression in the Acup group (Fig. 3C).

Acupuncture decreases TGF-β, IL-8, TNF-α and IL-1β expression in the CRF model rabbits via the TGF-β/Smad pathway. ELISA assays were performed to measure differences in TGF-β, IL-8, TNF-α and IL-1β concentrations in blood serum. The results revealed that the concentrations of TGF-β, IL-8, TNF-α and IL-1β in the model group were significantly increased when compared with those in the control group. Furthermore, the concentrations of TGF-β, IL-8, TNF-α and IL-1β in the Posi and Acup groups were significantly decreased relative to those in the model group. Finally, the concentrations of TGF-β, IL-8, TNF-α and IL-1β in the Acup+inhibitor group were significantly decreased relative to those in the Acup group (P<0.05 or P<0.01; Fig. 4).

Discussion

Renal interstitial fibrosis (RIF) is the main pathological change that occurs in various types of chronic kidney disease (CKD) and inevitably progresses to end-stage renal disease (ESRD) (28). The extent of RIF is correlated with the progression of renal disease (29). Therefore, it is important to alleviate any renal injury and its associated RIF. The

essence of renal insufficiency is the associated decrease in the glomerular filtration rate (GFR) (30). SCr and BUN levels are good indicators of GFR, and are widely used to evaluate renal function (31). In this study, the rabbits in the model group were gavaged with adenine for 3 weeks, and their body weight was significantly decreased. Moreover, the urine protein, and SCr and BUN levels in the model group were significantly higher than those in the control group. Therefore, it was demonstrated that the renal function of rabbits in the model group had been damaged, and the CRF model had been successfully constructed.

Acupuncture has been used as a complementary or alternative treatment for various diseases. However, to the best of our knowledge, there have been few reports of clinical trials that used acupuncture to treat CKD. Research has proven that stimulation of Zusanli (ST36) by electro-acupuncture (EA) can inhibit a reduction of endothelial nitric oxide synthase in the blood, reduce renal artery pressure, and protect kidney function (32). Furthermore, EA exerts an anti-inflammatory effect by reducing the levels of tumor necrosis factor-α (TNF-α) (33). Research has shown that periorbital acupuncture reduced the severity of a chemically induced renal injury in animals (34). More importantly, acupoint massage acts as a non-invasive technique that can boost energy levels, and improve an individual's health and comfort. For example, fatigue can be improved by massaging Yanglingchuan (GB34), Sanyinjiao (SP6) and Zusanli (35); sleep disturbances can be treated by Hand Shenmen (HT7) and Ear Shenmen (MATF1) (36); acupuncture or acupressure on Hegu (LI4) can relieve pain
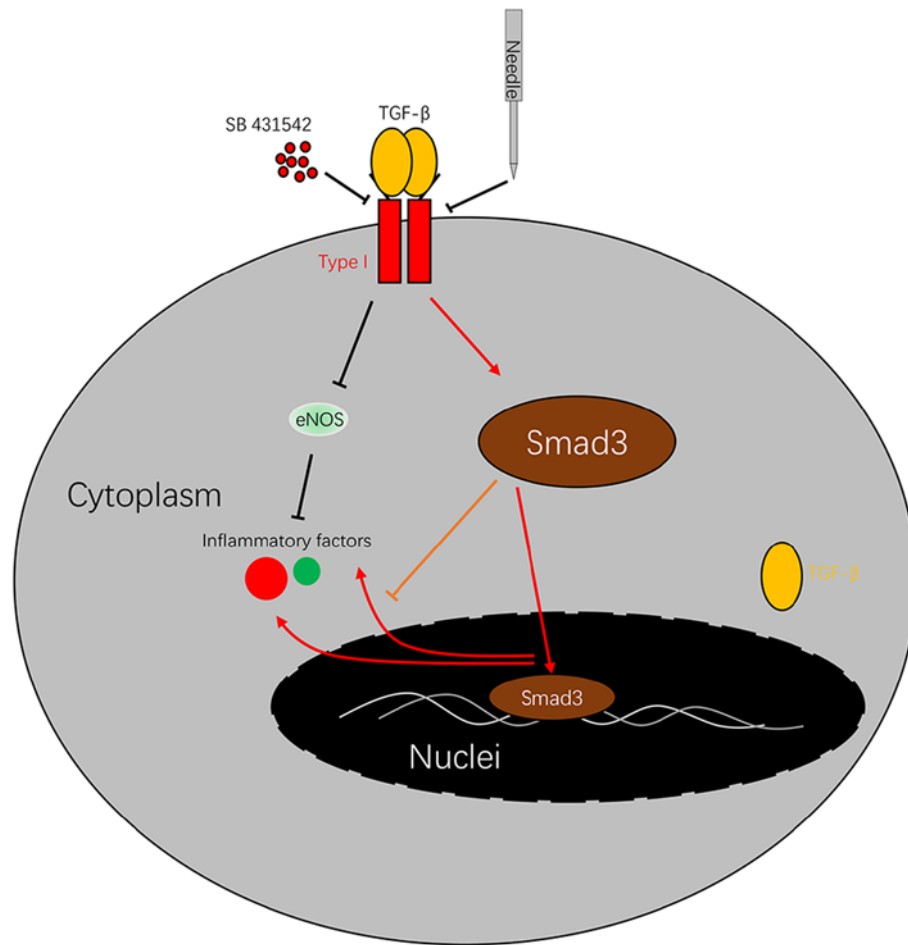
Figure 5. Schematic diagram of the present study. Acupuncture administration can block TGF-β signaling pathway, resulting in activated eNOS and inhibited Smad3 and attenuated inflammatory factors. TGF-β, transforming growth factor β; eNOS, endothelial nitric oxide synthase.

and exert anti-inflammatory effects (37); acupuncture on Taixi (KI3) can relieve renal disease, cognitive disorders and impotence (38). In this study, CRF rabbits were stimulated by acupuncture on Shenshu, Ming Men and Pishu, and also by Zusanli acupoint and Guanyuan point; after which, the effect on RIF was examined.

It is generally known that losartan potassium, an angiotensin II (Ang II) receptor antagonist, can disrupt the angiotensin system, and thereby reduce proteinuria and delay chronic renal dysfunction (39). In this study, losartan potassium was used as a positive control substance.

The development of RIF occurs in 4 phases: Modulation of cytokine expression; inflammatory cell infiltration; cell proliferation and epithelial-mesenchymal transition (EMT); and the ectopic accumulation of extracellular matrix (ECM) (40-42). During the development of RIF, EMT is defined as the process by which renal epithelial cells and fibroblasts become altered to form myofibroblasts (43). An abnormal accumulation of ECM is the main cause of RIF (44). In addition, fibroblasts, one of the main intrinsic cells in the renal interstitium, are the main cells that secrete ECM during the development of RIF (45,46). It has been demonstrated that the properties of fibroblasts become altered during the progression of RIF; these alterations include phenotypic changes, an abundant expression of α-SMA, increased fibroblast proliferation, and

an accumulation of interstitial ECM components such as type I collagen and fibronectin (46).

The TGF-β/Smad pathway plays a critical role in renal fibrosis and also inflammation. Researchers have suggested the TGF-β/Smad pathway as a potential therapeutic target for treating chronic kidney diseases (47). TGF-β plays a critical role in the RIF process by promoting expression of key components of the ECM (5,48). TGF-β can promote the synthesis of adhesive proteins, collagen, and the proteoglycans found in extracellular matrix; it can also attenuate the decrease in protease synthesis, prevent decomposition of newly synthesized ECM, disrupt the balance between ECM synthesis and degradation, and accelerate the development of RIF (48,49). TGF-β promotes fibrosis mainly via a signal transmitted by the downstream Smad family; related studies have shown that TGF-β/Smad signaling pathways play a key role in the pathogenesis of RIF (50,51). In addition, TGF-β can activate the mitogen activated protein kinase (MAPK) signal transduction pathway, which includes c-Jun N-terminal kinase (JNK), extracellular signal-regulated kinase (ERK), p38, and tumor necrosis factor-α (TNF-α) (52).

Integrins can interact with various cytoplasmic proteins including integrin-linked kinase (ILK), which transmits signals from the extracellular matrix to cells. ILK serves as a scaffolding protein, and helps to regulate functions involved in tissue regeneration, such as cell survival, actin

cytoskeleton dynamics and cell migration (53). A previous study demonstrated that ILK expression is required for TGF-β induction (54).

Endothelial nitric oxide synthase (eNOS) is a key enzyme involved in NO synthesis, which helps to regulate vascular physiology (55). Studies have confirmed that eNOS plays key roles in cell proliferation and migration (56). Previous research has shown that TGF-β partially regulates eNOS expression by promoting the binding of a nuclear factor to the eNOS promoter region (57). Another study revealed that TGF-β regulates eNOS which can be explained by the direct interaction between the eNOS promoter region and Smad2 (58). Moreover, the inflammation process can also be mediated by eNOS signaling (59).

In the present study, it was demonstrated that acupuncture downregulated TNF-α, Smad3, ILK and TGF-β expression, and upregulated eNOS expression in a CRF model by affecting the TGF-β/Smad pathway. SB 431542, a TGF-β inhibitor can block TGF-β and attenuate the release of inflammatory factors (Fig. 5). In addition, it was also shown that acupuncture decreased the levels of cytokines (IL-8, TNF-α and IL-1β) in a CRF model via the TGF-β/Smad pathway, suggesting that acupuncture can be used as an anti-inflammatory therapy.

In conclusion, a rabbit model of CRF was utilized to demonstrate that acupuncture can regulate TGF-β-related pathways such as TNF-α, Smad3, ILK and eNOS. Moreover, acupuncture decreased the levels of inflammation-associated cytokines, and attenuated RIF via the TGF-β/Smad pathway. These findings suggest that acupuncture can effectively reduce the typical kidney features of CRF, and promote the recovery of renal function by inhibiting the TGF-β/Smad pathway.

Acknowledgements

Availability of data and materials

All data generated or analyzed during this study are included in this published article.

Authors' contributions

ZZ and PDH completed the experimental design. ZZ, PDH, and YWJ performed most of the experiments with assistance from YZ. ZZ and PDH collected the data, and YZ and MSZ completed the data analysis. ZZ drafted the manuscript and MSZ revised it. All authors approved the manuscript before submission.

Ethics approval and consent to participate

All experiments were performed in accordance with the recommendations provided in Guidelines for the Care and Use of Laboratory Animals, and the study protocol was approved by the Animal Research Committee of Yunnan College of Traditional Chinese Medicine (Cumming, China).

Patient consent for publication

Not applicable.

Competing interests

The authors declare that they have no competing interests.

References

1. Alsahli M and Gerich JE: Hypoglycemia, chronic kidney disease, and diabetes mellitus. Mayo Clin Proc 89: 1564-1571, 2014.
2. Jha V, Garcia-Garcia G, Iseki K, Li Z, Naicker S, Plattner B, Saran R, Wang AY and Yang CW: Chronic kidney disease: Global dimension and perspectives. Lancet 382: 260-272, 2013.
3. Levey AS and Coresh J: Chronic kidney disease. Lancet 379: 165-180, 2012.
4. Hill NR, Fatoba ST, Oke JL, Hirst JA, O'Callaghan CA, Lasserson DS and Hobbs FD: Global prevalence of chronic kidney disease-a systematic review and meta-analysis. PLoS One 11: e0158765, 2016.
5. Farris AB and Colvin RB: Renal interstitial fibrosis: Mechanisms and evaluation. Curr Opin Nephrol Hypertens 21: 289-300, 2012.
6. Garber SL, Mirochnik Y, Brecklin CS, Unemori EN, Singh AK, Slobodskoy L, Grove BH, Arruda JA and Dunea G: Relaxin decreases renal interstitial fibrosis and slows progression of renal disease. Kidney Int 59: 876-882, 2001.
7. Lovisa S, LeBleu VS, Tampe B, Sugimoto H, Vadnagara K, Carstens JL, Wu CC, Hagos Y, Burckhardt BC, Pentcheva-Hoang T, *et al*: Epithelial-to-mesenchymal transition induces cell cycle arrest and parenchymal damage in renal fibrosis. Nat Med 21: 998-1009, 2015.
8. Xie XS, Zuo C, Zhang ZY, Liu HC, Feng SG, Zhang CL, Yuan W and Fan JM: Investigate the effects of compound radix notoginseng on renal interstitial fibrosis and kidney-targeting treatment. Sichuan Da Xue Xue Bao Yi Xue Ban 43: 28-33, 2012 (In Chinese).
9. Naito Y, Fujii A, Sawada H, Oboshi M, Iwasaku T, Okuhara Y, Morisawa D, Eguchi A, Hirotani S and Masuyama T: Association between renal iron accumulation and renal interstitial fibrosis in a rat model of chronic kidney disease. Hypertens Res 38: 463-470, 2015.
10. Menn-Josephy H, Lee CS, Nolin A, Christov M, Rybin DV, Weinberg JM, Henderson J, Bonegio R and Havasi A: Renal interstitial fibrosis: An imperfect predictor of kidney disease progression in some patient cohorts. Am J Nephrol 44: 289-299, 2016.
11. Lovisa S, Zeisberg M and Kalluri R: Partial epithelial-to-mesenchymal transition and other new mechanisms of kidney fibrosis. Trends Endocrinol Metab 27: 681-695, 2016.
12. He W, Dai C, Li Y, Zeng G, Monga SP and Liu Y: Wnt/beta-catenin signaling promotes renal interstitial fibrosis. J Am Soc Nephrol 20: 765-776, 2009.
13. Omori H, Kawada N, Inoue K, Ueda Y, Yamamoto R, Matsui I, Kaimori J, Takabatake Y, Moriyama T, Isaka Y and Rakugi H: Use of xanthine oxidase inhibitor febuxostat inhibits renal interstitial inflammation and fibrosis in unilateral ureteral obstructive nephropathy. Clin Exp Nephrol 16: 549-556, 2012.
14. Irita J, Okura T, Jotoku M, Nagao T, Enomoto D, Kurata M, Desilva VR, Miyoshi K, Matsui Y, Uede T, *et al*: Osteopontin deficiency protects against aldosterone-induced inflammation, oxidative stress, and interstitial fibrosis in the kidney. Am J Physiol Renal Physiol 301: F833-F844, 2011.
15. Tampe B and Zeisberg M: Evidence for the involvement of epigenetics in the progression of renal fibrogenesis. Nephrol Dial Transplant 29 (Suppl 1): i1-i8, 2014.
16. Meng XM, Tang PM, Li J and Lan HY: TGF-β/Smad signaling in renal fibrosis. Front Physiol 6: 82, 2015.
17. Heldin CH and Moustakas A: Role of Smads in TGFβ signaling. Cell Tissue Res 347: 21-36, 2012.

18. Macias MJ, Martin-Malpartida P and Massagué J: Structural determinants of Smad function in TGF-beta signaling. Trends Biochem Sci 40: 296-308, 2015.
19. Shi Y and Massagué J: Mechanisms of TGF-beta signaling from cell membrane to the nucleus. Cell 113: 685-700, 2003.
20. Hwangbo C, Tae N, Lee S, Kim O, Park OK, Kim J, Kwon SH and Lee JH: Syntenin regulates TGF-β1-induced Smad activation and the epithelial-to-mesenchymal transition by inhibiting caveolin-mediated TGF-β type I receptor internalization. Oncogene 35: 389-401, 2016.
21. Kang JS, Liu C and Derynck R: New regulatory mechanisms of TGF-beta receptor function. Trends Cell Biol 19: 385-394, 2009.
22. Zhuang Y, Xing JJ, Li J, Zeng BY and Liang FR: History of acupuncture research. Int Rev Neurobiol 111: 1-23, 2013.
23. Lan L, Zeng F, Liu GJ, Ying L, Wu X, Liu M and Liang FR: Acupuncture for functional dyspepsia. Cochrane Database Syst Rev: CD008487, 2014.
24. Haddad NE and Palesh O: Acupuncture in the treatment of cancer-related psychological symptoms. Integr Cancer Ther 13: 371-385, 2014.
25. Amezaga Urruela M and Suarez-Almazor ME: Acupuncture in the treatment of rheumatic diseases. Curr Rheumatol Rep 14: 589-597, 2012.
26. Li Z, Li M, Li X, Zhang M, Zhao Y, Ren W, Cheng J and Wang X: Hyperbaric oxygen inhibits venous neointimal hyperplasia following arteriovenous fistulization. Int J Mol Med 39: 1299-1306, 2017.
27. Livak KJ and Schmittgen TD: Analysis of relative gene expression data using real-time quantitative PCR and the 2(-Delta Delta C(T)) method. Methods 25: 402-408, 2001.
28. Chawla LS, Amdur RL, Amodeo S, Kimmel PL and Palant CE: The severity of acute kidney injury predicts progression to chronic kidney disease. Kidney Int 79: 1361-1369, 2011.
29. Muller GA, Markovic-Lipkovski J and Rodemann HP: The progression of renal diseases: On the pathogenesis of renal interstitial fibrosis. Klin Wochenschr 69: 576-586, 1991.
30. Mian AN and Schwartz GJ: Measurement and estimation of glomerular filtration rate in children. Adv Chronic Kidney Dis 24: 348-356, 2017.
31. Hall JA, Yerramilli M, Obare E, Yerramilli M, Yu S and Jewell DE: Comparison of serum concentrations of symmetric dimethylarginine and creatinine as kidney function biomarkers in healthy geriatric cats fed reduced protein foods enriched with fish oil, L-carnitine, and medium-chain triglycerides. Vet J 202: 588-596, 2014.
32. Kim DD, Pica AM, Durán RG and Durán WN: Acupuncture reduces experimental renovascular hypertension through mechanisms involving nitric oxide synthases. Microcirculation 13: 577-585, 2006.
33. Huang CL, Tsai PS, Wang TY, Yan LP, Xu HZ and Huang CJ: Acupuncture stimulation of ST36 (Zusanli) attenuates acute renal but not hepatic injury in lipopolysaccharide-stimulated rats. Anesth Analg 104: 646-654, 2007.
34. Liu J, Song KH, You MJ, Son DS, Cho SW and Kim DH: The effect of oculo-acupuncture on recovery from ethylene glycol-induced acute renal injury in dogs. Am J Chin Med 35: 241-250, 2007.
35. Tsay SL: Acupressure and fatigue in patients with end-stage renal disease-a randomized controlled trial. Int J Nurs Stud 41: 99-106, 2004.
36. Bender BG, Leung SB and Leung DY: Actigraphy assessment of sleep disturbance in patients with atopic dermatitis: An objective life quality measure. J Allergy Clin Immunol 111: 598-602, 2003.
37. Zhang SP, Yip TP and Li QS: Acupuncture treatment for plantar fasciitis: A randomized controlled trial with six months follow-up. Evid Based Complement Alternat Med 2011: 154108, 2011.
38. Chen S, Xu M, Li H, Liang J, Yin L, Liu X, Jia X, Zhu F, Wang D, Shi X and Zhao L: Acupuncture at the Taixi (KI3) acupoint activates cerebral neurons in elderly patients with mild cognitive impairment. Neural Regen Res 9: 1163-1168, 2014.
39. Li P, Chen YZ, Lin HL, Ni ZH, Zhan YL, Wang R, Yang HT, Fang JA, Wang NS, Li WG, et al: Abelmoschus manihot-a traditional Chinese medicine versus losartan potassium for treating IgA nephropathy: Study protocol for a randomized controlled trial. Trials 18: 170, 2017.
40. Cao Q, Harris DC and Wang Y: Macrophages in kidney injury, inflammation, and fibrosis. Physiology (Bethesda) 30: 183-194, 2015.
41. Meng XM, Nikolic-Paterson DJ and Lan HY: Inflammatory processes in renal fibrosis. Nat Rev Nephrol 10: 493-503, 2014.
42. Eddy AA: Overview of the cellular and molecular basis of kidney fibrosis. Kidney Int Suppl (2011) 4: 2-8, 2014.
43. Grande MT, Sánchez-Laorden B, López-Blau C, De Frutos CA, Boutet A, Arévalo M, Rowe RG, Weiss SJ, López-Novoa JM and Nieto MA: Snail1-induced partial epithelial-to-mesenchymal transition drives renal fibrosis in mice and can be targeted to reverse established disease. Nat Med 21: 989-997, 2015.
44. Genovese F, Manresa AA, Leeming DJ, Karsdal MA and Boor P: The extracellular matrix in the kidney: A source of novel non-invasive biomarkers of kidney fibrosis? Fibrogenesis Tissue Repair 7: 4, 2014.
45. Urban ML, Manenti L and Vaglio A: Fibrosis-a common pathway to organ injury and failure. N Engl J Med 373: 95-96, 2015.
46. Rockey DC, Bell PD and Hill JA: Fibrosis-a common pathway to organ injury and failure. N Engl J Med 373: 96, 2015.
47. Lan HY and Chung AC: TGF-β/Smad signaling in kidney disease. Semin Nephrol 32: 236-243, 2012.
48. Neelisetty S, Alford C, Reynolds K, Woodbury L, Nlandu-Khodo S, Yang H, Fogo AB, Hao CM, Harris RC, Zent R and Gewin L: Renal fibrosis is not reduced by blocking transforming growth factor-β signaling in matrix-producing interstitial cells. Kidney Int 88: 503-514, 2015.
49. Shen N, Lin H, Wu T, Wang D, Wang W, Xie H, Zhang J and Feng Z: Inhibition of TGF-β1-receptor posttranslational core fucosylation attenuates rat renal interstitial fibrosis. Kidney Int 84: 64-77, 2013.
50. Li J, Zhang Z, Wang D, Wang Y, Li Y and Wu G: TGF-beta 1/Smads signaling stimulates renal interstitial fibrosis in experimental AAN. J Recept Signal Transduct Res 29: 280-285, 2009.
51. Ning XH, Ge XF, Cui Y and An HX: Ulinastatin inhibits unilateral ureteral obstruction-induced renal interstitial fibrosis in rats via transforming growth factor β (TGF-β)/Smad signalling pathways. Int Immunopharmacol 15: 406-413, 2013.
52. He T, Bai X, Yang L, Fan L, Li Y, Su L, Gao J, Han S and Hu D: Loureirin B inhibits hypertrophic scar formation via inhibition of the TGF-β1-ERK/JNK pathway. Cell Physiol Biochem 37: 666-676, 2015.
53. Wickström SA, Lange A, Montanez E and Fässler R: The ILK/PINCH/parvin complex: The kinase is dead, long live the pseudokinase! EMBO J 29: 281-291, 2010.
54. Vi L, de Lasa C, DiGuglielmo GM and Dagnino L: Integrin-linked kinase is required for TGF-β1 induction of dermal myofibroblast differentiation. J Invest Dermatol 131: 586-593, 2011.
55. Su Y: Regulation of endothelial nitric oxide synthase activity by protein-protein interaction. Curr Pharm Des 20: 3514-3520, 2014.
56. García C, Nuñez-Anita RE, Thebault S, Arredondo Zamarripa D, Jeziorsky MC, Martínez de la Escalera G and Clapp C: Requirement of phosphorylatable endothelial nitric oxide synthase at Ser-1177 for vasoinhibin-mediated inhibition of endothelial cell migration and proliferation in vitro. Endocrine 45: 263-270, 2014.
57. Inoue N, Venema RC, Sayegh HS, Ohara Y, Murphy TJ and Harrison DG: Molecular regulation of the bovine endothelial cell nitric oxide synthase by transforming growth factor-beta 1. Arterioscler Thromb Vasc Biol 15: 1255-1261, 1995.
58. Saura M, Zaragoza C, Cao W, Bao C, Rodríguez-Puyol M, Rodríguez-Puyol D and Lowenstein CJ: Smad2 mediates transforming growth factor-beta induction of endothelial nitric oxide synthase expression. Circ Res 91: 806-813, 2002.
59. Paterniti I, Esposito E, Mazzon E, Bramanti P and Cuzzocrea S: Evidence for the role of PI(3)-kinase-AKT-eNOS signalling pathway in secondary inflammatory process after spinal cord compression injury in mice. Eur J Neurosci 33: 1411-1420, 2011.